Combined free and forced convection for developed flow in curved pipes with finite curvature ratio

Ru Yang and Sung Fa Chang
Institute of Mechanical Engineering, National Sun Yat-Sen University, Kaohsiung, Taiwan, Republic of China

Combined free and forced convection for developed flow in a curved pipe with arbitrary curvature ratio is studied numerically. The curved pipe is heated with axially uniform heat flux, while the wall temperature is maintained peripherally uniform. The buoyancy force is accounted by the Boussinesq approximation. The effects of the Dean, Prandtl, and Rayleigh numbers and especially of a wide range of curvature ratios on the flow resistance and the average heat transfer rate are presented. The significant distortion of the dividing streamline and the appearance of the secondary flow with one dominant cell for pipe flow with higher buoyancy force and curvature ratio are also discussed.

Keywords: curved pipe flow; buoyancy; arbitrary curvature ratio

Introduction

One prominent feature of the flow in a curved pipe is the appearance of a centrifugal-force-induced secondary flow present on the cross-sectional plane. In general, the existence of the secondary flow enhances heat and mass transfer rates and increases the skin friction. Dean (1927) was the first researcher for this problem who employed a perturbation technique to analyze secondary flow in a curved pipe. Thereafter, many studies on extending this topic by either theoretical or experimental means have been reported (Seban and McLaughlin 1963; Mori and Nakayama 1965; Truesdell and Adler 1970; Larrain and Bonilla 1970; Akiyama and Cheng 1971; Kalb and Seader 1972; Austin and Seader 1973; Patankar, Pratap, and Spalding 1974; Soh and Berger 1987; Yang and Chang 1993). A common assumption for most of the previous studies is that the momentum and energy equations are uncoupled. However, secondary flow can also be induced by a buoyancy force in heated curved pipe flows.

Morton (1959) showed that if a temperature distribution is present in a horizontal heated straight pipe, the varying gravitational force due to the difference in density causes a motion of fluid elements in the vertical direction. This effect forces secondary flow to form two vertical vortices with a vertical dividing streamline. Yao and Berger (1978) employed a perturbation method to analyze the influence of both centrifugal and buoyancy forces on the flow in heated curved pipes, and showed that the buoyancy effect can indeed be as important as the effect of the centrifugal force for small Dean number flows. Prusa and Yao (1982) numerically accounted for the combined effects of buoyancy and centrifugal forces in heated curved tubes with $O(\delta) \ll 1$, where δ is the curvature ratio of a curved pipe. They provided a flow-regime map to indicate the three basic regimes: (1) the regime with centrifugal force dominant, (2) the regime with both buoyancy and centrifugal force important, and (3) the regime with buoyancy force dominant. Lee et al. (1985) numerically studied the influence of buoyancy on fully developed laminar flow in curved tubes of circular cross section. They also presented a plot showing the relative importance of the buoyancy and the centrifugal effects. The aforementioned studies for buoyancy effect are restricted to small curvature ratio, δ. There remains to be studied the buoyancy effect in curved pipe flow with finite curvature ratio.

In addition, Cheng and Yuen (1987) reported a flow visualization on secondary flow patterns in a heated curved pipe by the smoke-injection method. They showed how the buoyancy and the curvature effects distort the dividing streamline of the secondary flow and the appearance of one dominant cell flow and a crescent region. They concluded that the symmetry of the secondary flow field can be maintained only when the viscosity effect is dominant over the body force effect. These phenomena have not yet been studied theoretically.

Therefore, the intention of the present work is to study, numerically, combined free and force convection for developed flow in heated curved pipes with arbitrary curvature ratio, especially for $\delta > 0.2$, and to demonstrate the existence of a dominant cell flow due to the increased buoyancy force and curvature ratio. Since curved pipe flow is widely employed in industrial heat exchangers, chemical reactors, and many other devices, the present work adds completeness to the study of the problem. A special application of this study is for improving solar-collector performance by using curved pipes.

Mathematical formulation

The physical problem considered in this study is a fully developed laminar incompressible flow in an axially uniformly heated curved pipe. Consequently, the pressure and the temperature gradients are constants along the main flow direction. The buoyancy force is accounted for by the

Address reprint requests to Professor Yang at the Institute of Mechanical Engineering, National Sun Yat-Sen University, Kaohsiung, Taiwan, Republic of China.

Received 3 February 1994; accepted 11 July 1994

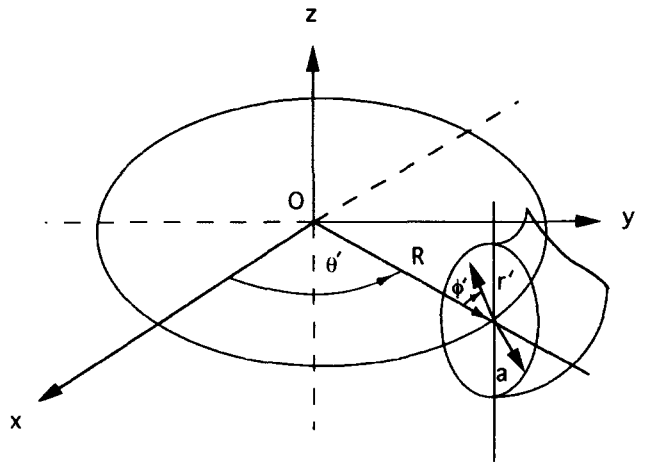

Figure 1 The physical coordinate system

Boussinesq approximation, and viscous dissipation is neglected. A suitable coordinate system for describing the problem is a curvilinear coordinate system (r', ϕ', θ') shown in Figure 1, and (u', v', w') are velocity components corresponding to (r', ϕ', θ') coordinates. The governing equations are

$$\nabla \cdot \vec{V} = 0$$

$$(\vec{V} \cdot \nabla)\vec{V} = -\frac{1}{\rho}\nabla P' + \nu \nabla^2 \vec{V} - \beta(T' - T'_w)\vec{g} \tag{1}$$

$$(\vec{V} \cdot \nabla)T' = \alpha \nabla^2 T'$$

The governing equations are nondimensionalized by defining the following dimensionless variables:

$$\delta = \frac{a}{R}, r = \frac{r'}{a}, \phi = \phi', \theta = \frac{\theta'}{\sqrt{\delta}}, u = \frac{u'}{\sqrt{\delta} w_c}, v = \frac{v'}{\sqrt{\delta} w_c}, w = \frac{w'}{w_c},$$

$$P = \frac{P'}{\rho w_c^2}, \mathrm{Re}_s = \frac{w_c a}{\nu}, \mathrm{De} = \delta \mathrm{Re}_s^2, T = \frac{T'_w - T'}{\tau a \mathrm{De}\,\mathrm{Pr}}, \mathrm{Ra} = \frac{\beta g \tau a^4}{\nu \alpha} \tag{2}$$

Notation

a Pipe radius
De Dean number, $\delta \mathrm{Re}_s^2$
f Friction factor
g Gravitational constant
G Axial pressure gradient, $-\frac{1}{R}\frac{\partial P'}{\partial \theta'}$
h Local heat transfer coefficient
$\bar{h}$ Mean heat transfer coefficient
k Fluid thermal conductivity
Nu Local Nusselt number, $\frac{2ah}{k}$
$\overline{\mathrm{Nu}}$ Peripherally average Nusselt number, $\frac{2a\bar{h}}{k}$
P Nondimensional pressure $P = \frac{P'}{\rho w_0^2}$
Pr Prandtl number, $\frac{\nu}{\alpha}$
Q Volumetric flow rate
R Radius of curvature
Ra Rayleigh number, $\frac{g\beta\tau a^4}{\nu\alpha}$
Re Reynolds number based on averaged axial velocity and pipe diameter
Re_s Reynolds number for corresponding straight pipe, $\frac{w_0 a}{\nu}$
T Dimensionless temperature, $\frac{T'_w - T'}{\tau a \mathrm{De}\,\mathrm{Pr}}$
u Dimensionless radial velocity, $\frac{u'}{\sqrt{\delta} w_0}$
v Dimensionless tangential velocity, $\frac{v'}{\sqrt{\delta} w_0}$
w Dimensionless axial velocity, $\frac{w'}{w_0}$
w_0 Centerline velocity of developed flow in a straight pipe with pressure gradient G, $\frac{Ga^2}{4\mu}$

Greek symbols

α Thermal diffusivity
β Coefficient of volumetric thermal expansion
δ Curvature ratio, a/R
θ Dimensionless angular coordinate in plane of pipe curvature, $\frac{\theta'}{\sqrt{\delta}}$
μ Dynamic viscosity
ν Kinematic viscosity
ρ Fluid density
τ Axial temperature gradient, $\frac{1}{R}\frac{\partial T'}{\partial \theta'}$
ϕ Angular coordinate in pipe cross section
ψ Dimensionless secondary-flow stream function
ω Dimensionless axial vorticity

Superscript

$'$ Dimensional variables

Subscripts

c Quantities associated with the curved pipe
s Quantities associated with the straight pipe

where $G = -\partial P'/R\partial\theta'$ and $\tau = \partial T'/R\partial\theta'$ are the constant pressure gradient and the temperature gradient along the axial direction respectively, and w_c and Re_s represent the maximum velocity and Reynolds number, respectively, for a fully developed flow in a corresponding straight pipe with the same pressure gradient G, and Ra and De are the Rayleigh number and the modified Dean number, respectively. The dimensionless governing equations are as follows:

Continuity:

$$\frac{\partial}{\partial r}[(1-\delta r\cos\phi)ru] + \frac{\partial}{\partial\phi}[(1-\delta r\cos\phi)v] = 0 \tag{3}$$

r—momentum:

$$u\frac{\partial u}{\partial r} + \frac{v}{r}\frac{\partial u}{\partial\phi} - \frac{v^2}{r} + \frac{w^2\cos\phi}{1-\delta r\cos\phi} = -\frac{1}{\delta}\frac{\partial P}{\partial r} - \frac{1}{\sqrt{\mathrm{De}}}\left[\left(\frac{1}{r}\frac{\partial}{\partial\phi} + \frac{\delta\sin\phi}{1-\delta r\cos\phi}\right)\left(\frac{v}{r} + \frac{\partial v}{\partial r} - \frac{1}{r}\frac{\partial u}{\partial\phi}\right)\right] - \mathrm{Ra}\,T\sin\phi \tag{4}$$

φ—momentum:

$$u\frac{\partial v}{\partial r} + \frac{v}{r}\frac{\partial v}{\partial\phi} + \frac{uv}{r} - \frac{w^2\sin\phi}{1-\delta r\cos\phi} = -\frac{1}{\delta r}\frac{\partial P}{\partial\phi} + \frac{1}{\sqrt{\mathrm{De}}}\left[\left(\frac{\partial}{\partial r} - \frac{\delta\cos\phi}{1-\delta r\cos\phi}\right)\left(\frac{v}{r} + \frac{\partial v}{\partial r} - \frac{1}{r}\frac{\partial u}{\partial\phi}\right)\right] - \mathrm{Ra}\,T\cos\phi \tag{5}$$

θ—momentum:

$$u\frac{\partial w}{\partial r} + \frac{v}{r}\frac{\partial w}{\partial\phi} - \frac{\delta w}{1-\delta r\cos\phi}(v\sin\phi - u\cos\phi) = \frac{4}{\sqrt{\mathrm{De}}(1-\delta r\cos\phi)} + \frac{1}{\sqrt{\mathrm{De}}}\left[\frac{1}{r}\frac{\partial}{\partial\phi}\left(\frac{1}{r}\frac{\partial w}{\partial\phi} + \frac{w\delta\sin\phi}{1-\delta r\cos\phi}\right) + \left(\frac{1}{r} + \frac{\partial}{\partial r}\right)\left(\frac{\partial w}{\partial r} - \frac{w\delta\cos\phi}{1-\delta r\cos\phi}\right)\right] \tag{6}$$

Energy:

$$u\frac{\partial T}{\partial r} + \frac{v}{r}\frac{\partial T}{\partial\phi} - \frac{w}{\mathrm{De}\,\mathrm{Pr}\sqrt{\delta}(1-\delta r\cos\phi)} = \frac{w}{\sqrt{\mathrm{De}}\,\mathrm{Pr}(1-\delta r\cos\phi)} \times\left[(1-\delta r\cos\phi)\left(\frac{\partial^2 T}{\partial r^2} + \frac{1}{r}\frac{\partial T}{\partial r} + \frac{1}{r^2}\frac{\partial^2 T}{\partial\phi^2}\right) + \delta\left(\frac{1}{r}\frac{\partial T}{\partial\phi}\sin\phi - \frac{\partial T}{\partial r}\cos\phi\right)\right] \tag{7}$$

A stream function ψ can be defined to satisfy Equation 3 by

$$u = \frac{1}{r(1-\delta r\cos\phi)}\frac{\partial\psi}{\partial\phi},\quad v = -\frac{1}{1-\delta r\cos\phi}\frac{\partial\psi}{\partial r} \tag{8}$$

and the dimensionless vorticity ω in the θ direction is defined as

$$\omega = \frac{v}{r} + \frac{\partial v}{\partial r} - \frac{1}{r}\frac{\partial u}{\partial\phi} \tag{9}$$

Then, by substituting ψ and ω into Equations 3 to 7 and eliminating the pressure terms in the r and ϕ momentum equations, one ends up with the following equations:

$$\left(\frac{\partial^2\psi}{\partial r^2} + \frac{1}{r}\frac{\partial\psi}{\partial r} + \frac{1}{r^2}\frac{\partial^2\psi}{\partial\phi^2}\right) - \frac{1}{1-\delta r\cos\phi}\left(\frac{\sin\phi}{r}\frac{\partial\psi}{\partial\phi} - \cos\phi\frac{\partial\psi}{\partial r}\right) + (1-\delta r\cos\phi)\omega = 0 \tag{10}$$

$$\left(\frac{\partial\psi}{\partial r}\frac{\partial\omega}{\partial\phi} - \frac{\partial\psi}{\partial\phi}\frac{\partial\omega}{\partial r}\right) + \omega\left(\frac{\partial^2\psi}{\partial r\partial\phi} - \frac{\delta r\sin\phi}{1-\delta r\cos\phi}\frac{\partial\psi}{\partial r}\right) + \frac{1}{1-\delta r\cos\phi}\left[\left(\frac{\partial^2\psi}{\partial r\partial\phi} + \frac{\delta\cos\phi}{1-\delta r\cos\phi}\frac{\partial\psi}{\partial\phi}\right)\left(\frac{\partial^2\psi}{\partial r^2} + \frac{1}{r^2}\frac{\partial^2\psi}{\partial\phi^2} + \frac{1}{1-\delta r\cos\phi}\frac{1}{r}\frac{\partial\psi}{\partial r} - \frac{\delta\cos\phi}{1-\delta r\cos\phi}\frac{1}{r}\frac{\partial\psi}{\partial\phi}\right)\right] + 2wr\left(\frac{\cos\phi}{r}\frac{\partial\psi}{\partial\phi} + \sin\phi\frac{\partial\psi}{\partial r}\right) = -\frac{1}{\sqrt{\mathrm{De}}} \times\left[\frac{r}{1-\delta r\cos\phi}\left(\frac{\partial^2\omega}{\partial r^2} + \frac{1}{r}\frac{\partial\omega}{\partial r} + \frac{1}{r^2}\frac{\partial^2\omega}{\partial\phi^2}\right) + \delta r\left(\frac{\sin\phi}{r}\frac{\partial\omega}{\partial\phi} - \cos\phi\frac{\partial\psi}{\partial r}\right) - \frac{\delta^2 r\omega}{1-\delta r\cos\phi}\right] - r\mathrm{Ra}\left(\frac{\sin\phi}{r}\frac{\partial T}{\partial\phi} - \cos\phi\frac{\partial T}{\partial r}\right) \tag{11}$$

$$\left(\frac{\partial w}{\partial r}\frac{\partial\psi}{\partial\phi} - \frac{\partial w}{\partial\phi}\frac{\partial\psi}{\partial r}\right) - \frac{\delta r w}{1-\delta r\cos\phi}\left(\frac{\cos\phi}{r}\frac{\partial\psi}{\partial\phi} + \sin\phi\frac{\partial\psi}{\partial r}\right) = \frac{1}{\sqrt{\mathrm{De}}}\left[\frac{r}{1-\delta r\cos\phi}\left(\frac{\partial^2 w}{\partial r^2} + \frac{1}{r}\frac{\partial w}{\partial r} + \frac{1}{r^2}\frac{\partial^2 w}{\partial\phi^2}\right) + \delta r\left(\frac{\sin\phi}{r}\frac{\partial w}{\partial\phi} - \cos\phi\frac{\partial w}{\partial r}\right) - \frac{\delta^2 r w}{1-\delta r\cos\phi} + 4r\right] \tag{12}$$

$$\left(\frac{\partial T}{\partial r}\frac{\partial\psi}{\partial\phi} - \frac{\partial T}{\partial\phi}\frac{\partial\psi}{\partial r}\right) - \frac{\delta r w}{\sqrt{\delta}\,\mathrm{De}\,\mathrm{Pr}} = \frac{1}{\sqrt{\mathrm{De}}\,\mathrm{Pr}}\left[\frac{r}{1-\delta r\cos\phi} \times\left(\frac{\partial^2 T}{\partial r^2} + \frac{1}{r}\frac{\partial T}{\partial r} + \frac{1}{r^2}\frac{\partial^2 T}{\partial\phi^2}\right) + \delta r\left(\frac{\sin\phi}{r}\frac{\partial T}{\partial\phi} - \cos\phi\frac{\partial T}{\partial r}\right)\right] \tag{13}$$

The boundary conditions are no-slip conditions on the wall, axially uniform heat flux, and peripherally uniform wall temperature, and the value of the stream function ψ on the wall is assigned to zero. The boundary condition for the vorticity ω can be derived from Equation 9. Therefore, the boundary conditions become the following:

$$r = 1:\ \psi = w = T = 0$$

$$\omega = -\frac{1}{1-\delta R\cos\phi}\frac{\partial^2\psi}{\partial r^2}\bigg|_{r=1} \tag{14}$$

The parameters present in the dimensionless governing equations are the curvature ratio (δ), the Dean number (De), the Rayleigh number (Ra), and the Prandtl number (Pr).

By following Soh and Berger (1987), the friction ratio can be defined as the ratio of the flow rate in a curved pipe to that in a straight pipe for the same pressure gradient, i.e.,

$$\frac{f_c}{f_s} = \frac{Q_s}{Q_c} = \frac{\pi}{2\int_0^{2\pi}\int_0^1 wr\,dr\,d\phi} \tag{15}$$

The mean peripheral Nusselt number is defined by

$$\overline{\mathrm{Nu}_c} = \frac{2a\bar{h}}{k} = \frac{\int_0^{2\pi} \mathrm{Nu}_c(1 - \delta\cos\phi)\,d\phi}{\int_0^{2\pi}(1 - \delta\cos\phi)\,d\phi} \tag{16}$$

where the local Nusselt number is defined as

$$\mathrm{Nu}_c = \frac{2ah}{k} = \frac{-2\left.\dfrac{\partial T}{\partial r}\right|_{r=1}}{T_m} \tag{17}$$

and T_m is the dimensionless bulk mean temperature defined as

$$T_m = \frac{\int_0^{2\pi}\int_0^1 Twr\,dr\,d\phi}{\int_0^{2\pi}\int_0^1 wr\,dr\,d\phi} \tag{18}$$

Numerical method

The governing equations are discretized into a set of finite-difference equations with a central-difference scheme. Since the dividing streamline between two vortices is generally distorted by the buoyancy effect, the horizontal line ($\phi = 0°$–$180°$) is no longer the symmetry line; therefore, the computational mesh should cover the entire cross section of the curved pipe. The grid number (25, 80) corresponding to (r, ϕ) is considered sufficient after several tests of different grid sizes.

The Gauss–Seidel iteration method is used for solving all governing equations. The straight-pipe parabolic velocity profile in the axial direction is employed as the initial guess, while other velocity components are set to zero initially. Also, low Dean-number flow solutions are used as the initial values for high Dean-number flow calculations in order to expedite the convergence rate. Underrelaxation is employed, and the relaxation factors are always between 0.5 to 0.8 for all governing equations. The convergence criterion is found to be sufficient when all relative errors of the dependent variables are less than 5×10^{-5}.

Results and discussion

The results of the combined free and forced convection in a curved pipe with finite curvature ratio are presented in terms of the friction ratio f_c/f_s and the heat transfer ratio $\overline{\mathrm{Nu}_c}/\overline{\mathrm{Nu}_s}$. The secondary flow patterns and the profiles of the axial velocity and temperature are also of interest.

Results for the friction ratio

Without buoyancy considerations, the results of the friction ratio for a curved pipe flow with finite curvature ratio have been reported by Larrain and Bonilla (1970), Austin and Seader (1973), Soh and Berger (1987), and Yang and Chang (1993). Figure 2 shows excellent agreement in its comparison of the present results of the friction ratio with those of the previous studies for the cases without buoyancy effects (Ra = 0). It is clearly shown in Figure 2 that the friction ratio becomes larger, as expected, when the buoyancy effect is taken into account (Ra > 0). This increase of the friction ratio by the buoyancy effect becomes less prominent when the flow Dean number becomes sufficiently large that the centrifugal force becomes dominant over the buoyancy force. A larger curvature ratio enhances the secondary flow but also increases the friction ratio, as shown in Figure 3. Figures 2 and 3 also show that the friction ratio increases with an increased Dean number.

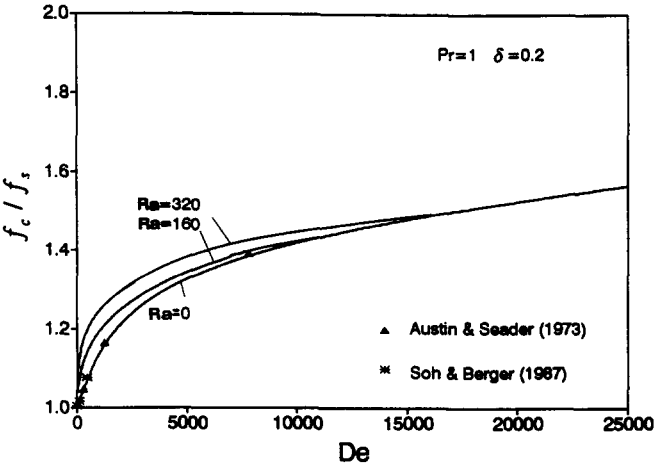

Figure 2 Variation of friction factor ratio with De and Ra

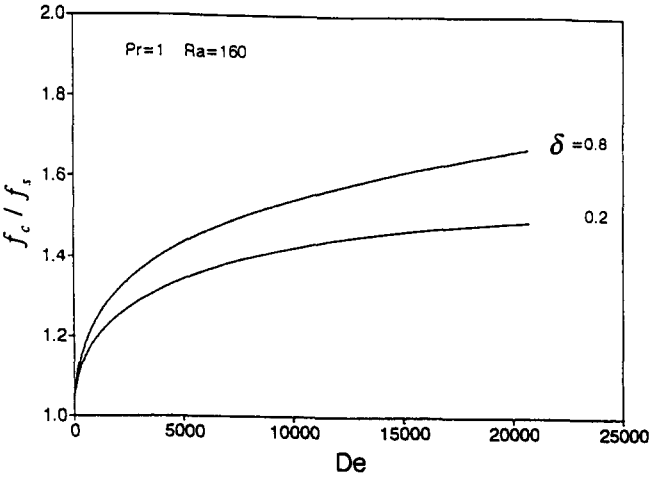

Figure 3 Variation of friction factor ratio with De and δ

Results for the secondary flow pattern

Figure 4 shows the effects of the Rayleigh number and the curvature ratio on the secondary flow pattern. In Figure 4, the left-hand side represents the inner wall of the curved pipe, and the right-hand side represents the outer wall. Three values of the curvature ratio (δ = 0.1, 0.25, and 0.8) and three values of Rayleigh number (Ra = 0, 40, and 80) are shown for the case in which De = 100 and Pr = 1. The case in which Ra = 0 corresponds to an unheated flow, and the secondary flow is induced solely by centrifugal force. When Ra = 40, both centrifugal and buoyancy forces are present. The dividing streamline is distorted toward the lower portion of the pipe when the curvature ratio is increased. It can also be seen that the upper cell becomes the dominant flow region when δ = 0.8. Note that the values of stream function are equally spaced in the figure. Consequently, the dense streamlines of the upper cell mean that the flow is faster, while the sparse streamlines of the lower cell correspond to a slower flow. Thus, the secondary flow has only one cell (the upper cell) dominant. When Ra = 80, the secondary flow field is more dominated by the buoyancy effect. The dividing streamline is more distorted, and the secondary flow with one dominant cell is more obvious. This phenomenon is qualitatively in accord with the experimental observation made by Cheng and Yuen (1987), and has not been reported theoretically owing to the restricted small

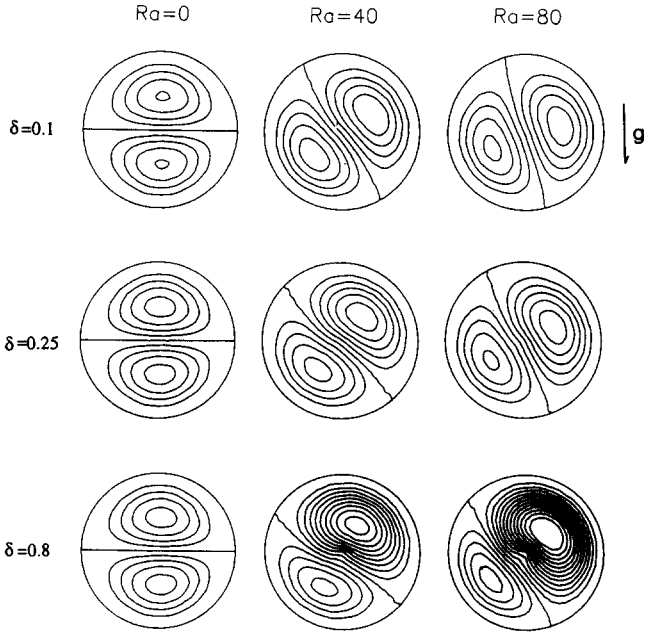

Figure 4 Secondary flow patterns for various Ra and δ (De = 100, Pr = 1)

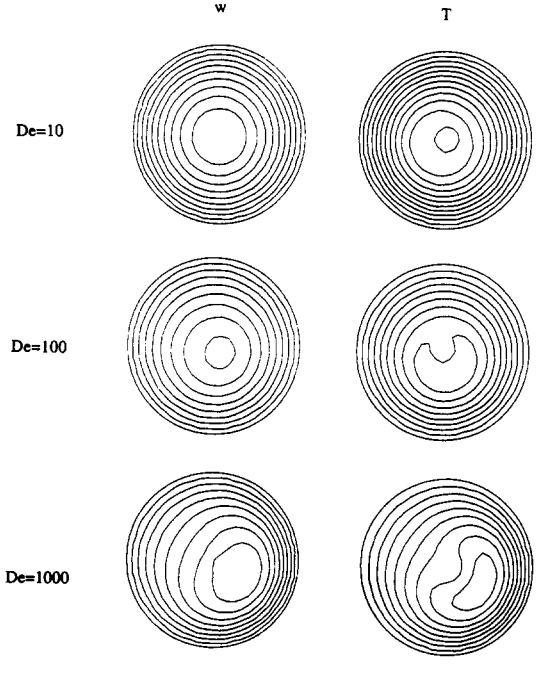

Figure 5 Axial velocity and temperature contours for various De (Ra = 40, Pr = 1, δ = 0.1)

curvature ratio imposed in previous numerical studies. The crescent region appearing in Chang and Yuen's photograph should be the lower cell, which flows much more slowly than does the upper cell.

Results for the main flow

It is well known that due to centrifugal force induced by the pipe curvature, the maximum axial velocity is displaced from the central axis of the pipe toward the outer wall (ϕ = 180°). However, when the pipe is heated, the combined effects of buoyancy and centrifugal forces will rotate the contour of the axial velocity. In Figure 5, where Ra = 40, δ = 0.1, Pr = 1, and De = 10, the centrifugal force is very small, so the contour of the axial velocity is similar to that of a straight-tube flow. For De = 100, the centrigual force starts to shift the position of the maximum axial velocity. When De = 1,000, the combined effect of the buoyancy force and centrifugal force is very obvious in that the position of the maximum axial velocity has been displaced to the southeast corner of the pipe. The contour is almost symmetric about the line ϕ = 25°–225°, which indicates that the dividing streamline of the secondary flow lies approximately on this line.

Results for the temperature field

The effects of the buoyancy force and the centrifugal force on the temperature profiles are similar to those on the axial velocity profiles, and are shown in Figure 5. The other explicit parameter that affects the profiles of temperature field is the Prandtl number. As the Prandtl number becomes larger, the convection is more dominant, and the thermal boundary layer becomes thinner near the pipe wall. These phenomena are shown in Figure 6. A detailed discussion of the Pr effect has been given by Lee et al. (1985).

Results for the heat transfer ratio

The effects of Ra on the heat transfer ratio, $\overline{Nu_c}/\overline{Nu_s}$, are shown in Figure 7. The heat transfer ratio is shown to increase with the increased buoyancy effect. Also shown in this figure is that the heat transfer ratio becomes independent of the buoyancy force when the flow Dean number is high, and axial convection is dominant over transverse convection. On the other hand, Figure 8 shows that the heat transfer ratio decreases with increasing curvature ratio. The reason is that for the same Dean number (δRe_s^2), a higher δ corresponds to a slower main flow, which results in a lower axial convective heat transfer rate. Figure 9 shows the effect of the Prandtl number on the heat transfer ratio. The heat transfer ratio is much higher for a high Pr fluid.

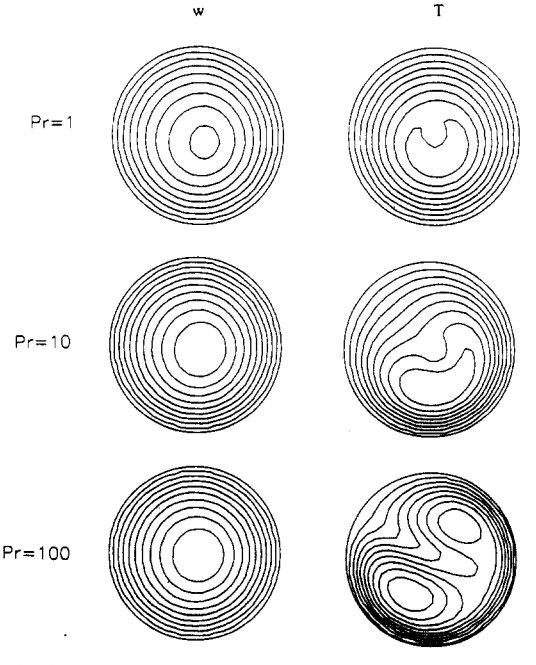

Figure 6 Axial velocity and temperature contours for various Pr (De = 100, Ra = 40, δ = 0.1)

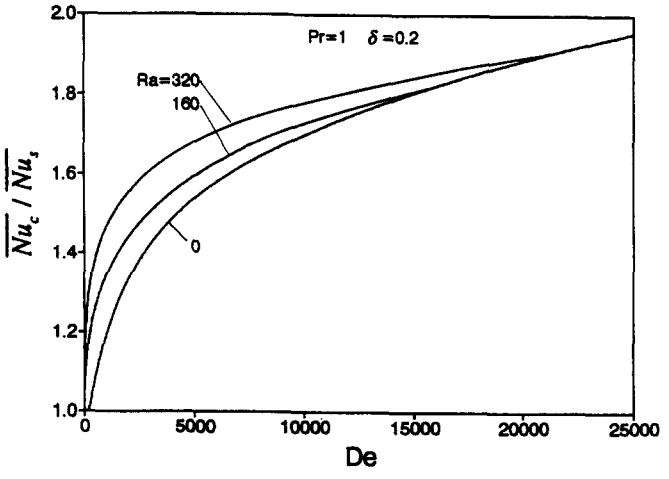

Figure 7 Variation of average Nusselt number ratio with De and Ra

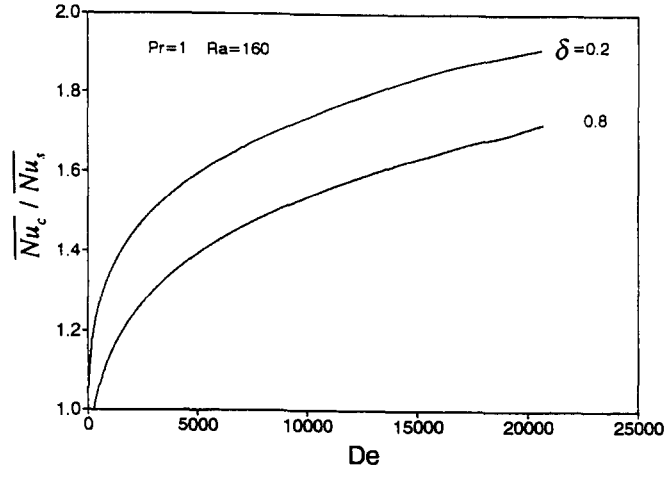

Figure 8 Variation of average Nusselt number ratio with De and δ

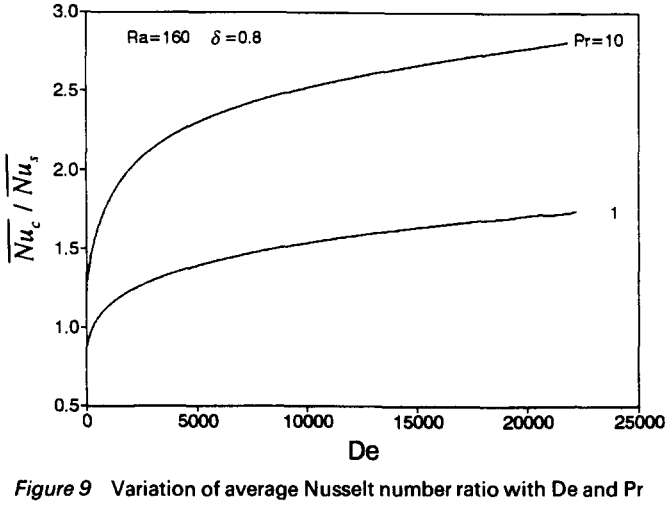

Figure 9 Variation of average Nusselt number ratio with De and Pr

Conclusions

The present numerical study extends the previous works in the literature for the flow and heat transfer in a heated curved pipe by liberating the small curvature restriction and including the effect of the buoyancy force. The previous experimental observation of the one-cell dominated secondary flow and the presence of the crescent region for a flow with high curvature ratio and buoyancy effect is predictable by the present calculation. The ranges of the parameters in this study are Dean number from 10 to 25,000, Prandtl number from 0.7 to 100, Rayleigh number from 0 to 320, and curvature ratio from 0.01 to 0.8. The friction ratio is found to increase with increasing curvature ratio and buoyancy effect, while, on the other hand, the heat transfer ratio increases with increasing buoyancy effect but decreases with increasing curvature ratio. Both heat transfer and friction ratio increase with increasing Dean number. The present study suggests the following correlations:

$$\frac{f_c}{f_s} = 0.689\mathrm{De}^{0.0817}\mathrm{Pr}^{0.0081}\mathrm{Ra}^{0.0068}\delta^{0.0084}$$

$$\frac{\overline{\mathrm{Nu}_c}}{\overline{\mathrm{Nu}_s}} = 0.42\mathrm{De}^{0.111}\mathrm{Pr}^{0.21}\mathrm{Ra}^{0.0513}\delta^{-0.0974}$$

$$\frac{\overline{\mathrm{Nu}_c}/\overline{\mathrm{Nu}_s}}{f_c/f_s} = 0.61\mathrm{De}^{0.0293}\mathrm{Pr}^{0.202}\mathrm{Ra}^{0.0445}\delta^{-0.106}$$

The correlation coefficients, R^2, are 0.932, 0.985, and 0.973, respectively.

Acknowledgment

This work was partly sponsored by the National Science Council, Taiwan, Republic of China, under the contract NSC 81-0115-C110-01-029E.

References

Akiyama, M. and Cheng, K. C. 1971. Boundary vorticity method for laminar forced convection heat transfer in curved pipes. *Int. J. Heat Mass Transfer*, **14**, 1659–1675

Austin, L. R. and Seader, J. D. 1973. Fully developed viscous flow in coiled circular pipes. *AIChE J.*, **19**, 85–94

Berger, S. A., Talbot, L., and Yao, L. S. 1983. Flow in curved pipe. *Annu. Rev. Fluid Mech.*, **15**, 461–512

Cheng, K. C. and Yuen, F. P. 1987. Flow visualization experiments on secondary flow patterns in an isothermally heated curved pipe. *J. Heat Transfer*, **109**, 55–61

Dean, W. R. 1927. Note on the motion of fluid in a curved pipe. *Philos. Mag.*, **20**, 208–223

Futagami, K. and Aoyama, Y. 1988. Laminar heat transfer in a helically coiled tube. *Int. J. Heat Mass Transfer*, **31**, 387–396

Kakac, S., Shah, R. A., and Aung, W. 1987. *Handbook of Single-Phase Convective Heat Transfer*, Wiley, New York, Chapter 5

Kalb, C. E. and Seader, J. D. 1972. Heat and mass transfer phenomena for viscous flow in curved circular tubes. *Int. J. Heat Mass Transfer*, **15**, 801–817

Larrain, J. and Bonilla, C. F. 1970. Theoretical analysis of pressure drop in the laminar flow of fluid in a coiled pipe. *Trans. Soc. Rheol.*, **14**, 135–147

Lee, J.-B., Simon, H. A., and Chow, J. C. F. 1985. Buoyancy in developed laminar curved tube flows. *Int. J. Heat Mass Transfer*, **28**, 631–640

Mori, Y. and Nakayama, W. 1965. Study on forced convective heat transfer in curved pipes. *Int. J. Heat Mass Transfer*, **8**, 67–82

Morton, B. R. 1959. Laminar convection in a uniformly heated horizontal pipe at low Rayleigh numbers. *Q. J. Mech. Appl. Math.*, **12**, 410–420

Patankar, S. V., Pratap, V. S., and Spalding, D. B. 1974. Prediction of laminar flow and heat transfer in helically coiled pipes. *J. Fluid Mech.*, **62**, 539–551

Pedley, T. J. 1980. *The Fluid Mechanics of Large Blood Vessels*. Cambridge University Press, Cambridge, 160–234

Prusa, J. and Yao, L. S. 1982. Numerical solution for fully developed flow in heated curved tubes. *J. Fluid Mech.*, **123**, 503–522

Seban, R. A. and McLaughlin, E. F. 1963. Heat transfer in tube coils with laminar and turbulent flow. *Int. J. Heat Mass Transfer*, **6**, 387–395

Soh, W. Y. and Berger, S. A. 1987. Fully developed flow in a curved pipe of arbitrary curvature ratio. *Int. J. Numer. Methods Fluids*, **7**, 733–755

Topakoglu, H. C. 1967. Steady laminar flows of an incompressible viscous fluid in curved pipes. *J. Math. Mech.*, **16**, 1321–1328

Truesdell, L. C. and Adler, R. J. 1970. Numerical treatment of fully developed laminar flow in helically coiled tubes. *AIChE J.*, **16**, 1010–1015

Yang, R. and Chang, S. F. 1993. A numerical study of fully developed laminar flow and heat transfer in a curved pipe with arbitrary curvature ratio. *Int. J. Heat Fluid Flow*, **14**, 138–145

Yao, L. S. and Berger, S. A. 1978. Flow in heated curved pipes. *J. Fluid Mech.*, **88**, 339–354